Prolonged DNA Damage Checkpoint Arrest Requires Constant Renewal and the Spindle Assembly Checkpoint

Felix Y. Zhou[1]*, David P. Waterman[2]*, Suhaily Caban-Penix[1], Vinay V. Eapen[3], and James E. Haber[1#]

[1] Department of Biology and Rosenstiel Basic Medical Sciences Research Center, Brandeis University, Waltham, MA 02453, USA

Current address:

[2] Prime Medicine Inc, 21 Erie St, Cambridge, MA 02139, USA

[3] Casma Therapeutics, 400 Technology Square Suite 201, Cambridge, MA 02139, USA

* These authors contributed equally to this work

To whom correspondence should be addressed. haber@brandeis.edu

Abstract

To prevent cell division in the presence of a DNA double-strand breaks (DSB), cell cycle progression is arrested by the DNA damage checkpoint (DDC) to allow more time for repair. In budding yeast, a single irreparable DSB arrests cells for about 12 h – 6 normal doubling times - after which cells adapt to the damage and resume the cell cycle. In contrast, 2 DSBs provoke permanent G_2/M arrest. While activation of the DDC is well-understood, how it is maintained remains unclear. To address this question, key checkpoint proteins were inactivated by auxin-inducible degradation 4 h after damage induction. Degradation of Ddc2^{ATRIP}, Rad9, Rad24, or Rad53^{CHK2} resulted in resumption of cell cycle, indicating that these checkpoint factors are required both to establish and to maintain DDC arrest. However, when Ddc2 is inactivated 15 h after inducing 2 DSBs, cells remain arrested. This continued arrest depends on the spindle-assembly checkpoint (SAC) proteins Mad1, Mad2, and Bub2. Although Bub2 acts with Bfa1 to regulate mitotic exit, inactivation of Bfa1 did not trigger checkpoint release. These data suggest that prolonged cell cycle arrest in response to 2 DSBs is achieved by a handoff from the DDC to specific components of the SAC.

Introduction

DNA double-strand breaks (DSBs) are one of the most deleterious forms of DNA damage. The DNA damage checkpoint (DDC) blocks cell cycle progression by halting the transition from metaphase to anaphase (known as the G_2/M checkpoint), giving cells an extended opportunity to repair DSBs. The G_2/M checkpoint prevents the inheritance of broken chromosomes, which can lead to aneuploidy and chromosome aberrations (Lanz et al., 2019; Waterman et al., 2020).

In budding yeast, a single irreparable DSB activates the DDC through the activity of Mec1,

a PI3K-like kinase and homolog of the mammalian ATR kinase (Mantiero et al., 2007; Pellicioli et al., 2001). Activation of Mec1 occurs following 5' to 3' resection of the DSB ends that creates single-stranded DNA (ssDNA), which is initially bound by the ssDNA binding complex, RPA (reviewed in (Marechal and Zou, 2015). Mec1 binds to ssDNA via its obligate binding partner, $Ddc2^{ATRIP}$ (Dubrana et al., 2007; Zou and Elledge, 2003). Additionally, the PCNA-related 9-1-1 clamp, made up of proteins Ddc1, Rad17, and Mec3, is loaded at the resected ss/dsDNA junction by the Rad24-Rfc2-5 clamp loader (Ellison and Stillman, 2003; Majka et al., 2006). The Ddc1 subunit of the 9-1-1 clamp then facilitates Mec1's kinase activity (Melo et al., 2001; Navadgi-Patil and Burgers, 2009). In contrast, yeast's other PI3K-like kinase, Tel1, the homolog of mammalian ATM, is dispensable for DDC activation, but its deletion shortens arrest by a few hours (Dubrana et al., 2007).

Maintenance of the DDC signaling requires continual Mec1 activity. Inhibition of Mec1, either by the checkpoint inhibitor caffeine or by using temperature-sensitive Mec1 mutants rapidly extinguishes checkpoint signaling (Pellicioli et al., 2001; Tsabar et al., 2015; Vaze et al., 2002). Numerous proteins are phosphorylated either directly by Mec1 or by the downstream effector kinases Rad53 and Chk1 (human CHK2 and CHK1), which are themselves Mec1 substrates. Mec1 and Tel1 phosphorylate histone H2A-S129, γH2AX, outwards from the DSB site (Li et al., 2020) which then recruits the scaffold protein Rad9. Mec1-phosphorylated Rad9 recruits Rad53 (Durocher et al., 1999; Emili, 1998; Schwartz et al., 2002). Rad53 then amplifies the checkpoint signal through autophosphorylation in *trans*, activating the Dun1 kinase transcription regulator, and restraining degradation of Pds1 (securin) (Chen et al., 2007; Fiorani et al., 2008; Pellicioli et al., 1999; Usui and Petrini, 2007; Yam et al., 2020).

In addition to the DDC, genomic integrity is also maintained by the spindle assembly

checkpoint (SAC) in response to unattached kinetochores (reviewed by (Musacchio and Salmon, 2007). Several studies have demonstrated connections between the DDC and the spindle assembly checkpoint (SAC). When exposed to DNA damaging agents such as hydroxyurea (HU) or methyl methanesulfonate (MMS), deletion of the SAC genes *MAD1* or *MAD2,* along with double deletions of the DDC genes *RAD9* and *RAD24*, resulted in a checkpoint response that was shorter than the double deletion of *RAD9* and *RAD24* (Garber and Rine, 2002; Kim and Burke, 2008). Furthermore, cells lacking *MAD1, MAD2* or *BUB1* arrest for a shorter length of time than wild type cells following induction of a DSB (Dotiwala et al., 2010). In mouse oocytes, inhibition of the SAC overrides activation of DDC-mediated metaphase arrest during the first meiotic division (Marangos et al., 2015).

Here we present new insights into maintenance of the DNA damage checkpoint (DDC) by using auxin-inducible degron (AID) tags to degrade checkpoint proteins after the establishment of the DDC. An advantage of the AID system compared to deletion and temperature-sensitive mutants is that AID-tagged proteins can retain wildtype function until the addition of the plant hormone auxin (IAA), which triggers rapid degradation of AID-tagged proteins in the presence of the TIR1 E3 ubiquitin ligase (Morawska and Ulrich, 2013; Nishimura et al., 2009). We found that checkpoint arrest in response to DSBs requires the constant presence of some, but not all, checkpoint activation proteins. We also showed that there is a handoff of checkpoint arrest between the DDC and the SAC, which was dependent on the SAC proteins Mad1, Mad2, and Bub2, but not Bub2's partner, Bfa1.

Results

Measuring DNA damage checkpoint arrest and maintenance

To measure the role of checkpoint activation proteins in the maintenance of the DNA damage checkpoint (DDC), we utilized a modified version of the well-characterized strain JKM179 and the auxin-inducible degron (AID) system (Nishimura et al., 2009). In these strains HO endonuclease, expressed from a *GAL1/10* promotor (*GAL-HO*), was induced to make a site-specific DSB in the *MAT* locus on chromosome III and/or at an introduced cleavage site located 52 kb from the centromere on chromosome IV (Kim et al., 2007; Lee et al., 1998). Cutting by HO after galactose induction is nearly complete at both sites within 30-45 minutes (Lee et al., 2014). To prevent repair by homologous recombination, the *HML* or *HMR* donors were deleted. Repair of a continuously induced HO-induced DSB via nonhomologous end-joining occurs in only 0.2% of cells (Moore and Haber, 1996).

In budding yeast, checkpoint arrest by the DDC will cause cells to shift into G_2/M arrest, which is seen as a large-budded cell with a single DAPI-staining nucleus (**Figure S1**). DSB-induced cell cycle arrest was monitored in 4 ways: (1) an adaptation assay where individual G1 cells are microscopically monitored on YEP-Gal agar plates (Lee et al., 1998), (2) monitoring the percentage of G2/M-arrested cells based on cell morphology in liquid culture, (3) monitoring nuclear division at mitosis by DAPI staining of nuclei, and (4) measuring Rad53 phosphorylation by western blot (Pellicioli et al., 2001).

In both the 1-DSB and 2-DSB strains, within 4 h after adding galactose to induce HO in liquid culture or after placed on a YEP-Gal plate, adaptation assays and DAPI staining showed that 83-98% of cells shifted towards G_2/M arrest (**Figure 1**). In addition, western blot analysis showed that Rad53 was hyperphosphorylated in both backgrounds 4 h after DSB induction (**Figure 1B, E**). In the 1-DSB strain, following G1 cells micromanipulated on plates, cells began to escape G_2/M arrest 12-15 h after DSB induction and only 2% of cells remained in a large-budded state by

24 h (**Figure 1A, C**). Dephosphorylation of Rad53 in the 1-DSB background was correlated with the escape from G_2/M arrest (**Figure 1B**). However, in the 2-DSB background over 90% of cells remained in G_2/M arrest as shown by the adaptation assay and by DAPI staining (**Figure 1D, F**). The creation of two DSBs extends DDC arrest past the point of adaptation seen in a 1-DSB strain (Lee et al., 1998) and allowed us to better study how the checkpoint is maintained. Unless otherwise stated, all strains discussed are in the 2-DSB background.

Analysis of checkpoint factors required for checkpoint maintenance

We used to AID system to degrade checkpoint proteins after G_2/M arrest was established. Since checkpoint arrest in budding yeast is primarily controlled by the kinase Mec1 (Clemenson and Marsolier-Kergoat, 2009), we appended an AID tag with 9 copies of the c-MYC epitope tag to the C-terminus of the checkpoint factors Ddc2, Rad9, Rad24, and Rad53 which are all part of the Mec1 pathway (de la Torre-Ruiz et al., 1998; Memisoglu et al., 2019; Sweeney et al., 2005). Hereafter, Ddc2-9xMyc-AID and other AID-tagged proteins will be designated simply as -AID, e.g. Ddc2-9xMyc-AID as Ddc2-AID.

Adding the AID tags did not affect the establishment of G_2/M arrest, but Rad9-AID, Rad24-AID, and Rad53-AID proved to be "leaky" and adapted after 24 h on a YEP-Gal plate (**Figure S2A-B**); this escape was dependent on the presence of TIR1 and reflects the presence of IAA as a natural biosynthetic intermediate in amino acid biosynthesis. When 1 mM IAA was added 2 h prior to Gal-HO induction, G_2/M arrest was largely prevented (**Figure S3A**), AID-tagged proteins were rapidly degraded as shown by western blot analysis (**Figure S3C-F**), and Rad53 hyper phosphorylation was nearly absent (**Figure S3B-F**); however, there was some residual arrest that was not seen in full deletion mutations of Rad9 or Rad53 (Dotiwala et al., 2010). Because

these constructs largely maintained arrest in the absence of IAA at 4 h, we could ascertain the effect of depleting these proteins at that time.

To examine the role of DDC proteins in the maintenance of the checkpoint, cultures were split 4 h after Gal-HO induction and treated with either 1 mM IAA or an equivalent volume of ethanol. Ddc2-AID, Rad9-AID, or Rad24-AID all arrested 4 h after Gal-HO induction, with 89%, 99%, or 99% of cells arrested in G_2/M, respectively (**Figure 2A-C**). Western blot analysis showed that 1 h after the addition of IAA, Ddc2-AID, Rad9-AID, or Rad24-AID were largely degraded and Rad53 began to lose phosphorylation (**Figure 2A-C)**. Degradation of the AID-tagged checkpoint proteins triggered release from G_2/M arrest; 1 h after the addition of IAA, the percentage of arrested cells decreased ~60%. DAPI staining of Ddc2-AID cells 1 h after IAA addition revealed large-budded cells with 2 distinct DAPI signals indicating cells had progressed into anaphase (**Figure S4A**).

When Rad53-AID was examined, despite rapid IAA-induced degradation of the tagged protein, cells remained in G_2/M arrest for ≥ 4 h (**Figure 2D**) and DAPI staining showed cell populations slowly transition into anaphase (**Figure S4B**). This delay in checkpoint release could be due to continued activity from downstream targets of Rad53 or from other targets of the Mec1 kinase, dependent on Ddc2, Rad9 and Rad24.

Chk1 sustains checkpoint signaling in the absence of Ddc2, Rad9, Rad24, or Rad53

Since Rad53 and Chk1 kinases both contribute to cell cycle arrest after DNA damage (Dotiwala et al., 2007; Pellicioli et al., 2001), we examined whether the 4 h delay in checkpoint release following Rad53-AID degradation was due to Chk1 signaling. Deleting *CHK1* in the 2-DSB strain did not affect establishment of arrest; cells remained arrested for at least 7 h. However, by 24 h,

>95% of *chk1*Δ cells adapted (**Figure 3A-B**). Although *chk1*Δ cells eventually overcome G_2/M arrest and adapt with 2 DSBs, the fact that they remain arrested for > 7 h allowed us to examine Chk1's role in maintaining checkpoint signaling in the absence of Rad53.

We deleted *CHK1* in the Rad53-AID strain and monitored checkpoint arrest as before. Rad53-AID *chk1*Δ readily escaped arrest when IAA was added to cultures 4 h after DSB induction; G_2/M cells dropped from 86% to 64% after 1 h (**Figure 3C)** (compare with *CHK1* Rad53-AID cells shown in Figure 2D). These results suggest that Chk1 is responsible for the sustained checkpoint arrest when Rad53-AID is degraded. Since Chk1 contributed to checkpoint maintenance when Rad53-AID was degraded, we asked whether Chk1 also contributed to the persistence of G_2/M cells when the other AID-tagged checkpoint proteins were degraded. The percentage of large-budded cells in *chk1*Δ derivatives of Ddc2-AID, Rad9-AID, and Rad24-AID returned to baseline levels within 2 h after adding IAA (**Figure 3D-F, Table S1**). Taken together, these results suggest that Chk1 is not required for the activation of the DDC but does contribute to checkpoint maintenance.

Previous studies have shown that Chk1 is phosphorylated both by Tel1 and Mec1 (Limbo et al., 2011; Sanchez et al., 1999). We therefore examined the effect of Tel1 in checkpoint maintenance. Unlike *chk1*Δ, with 2 DSBs, a *TEL1* deletion did not affect either the establishment of the DDC or the maintenance of checkpoint arrest up to 24 h (**Figure S5**). This result suggests that Mec1-mediated activation of Rad53 and Chk1 is sufficient for both checkpoint activation and maintenance as observed through these assays.

Dun1 is required for checkpoint activation but not maintenance

We entertained the idea that Rad53 switches on the expression of other proteins that could sustain

arrest after Rad53 activity was abolished. One candidate for this activity was Dun1, a protein kinase that regulates damage-related transcription (Chen et al., 2007; Yam et al., 2020; Zhou and Elledge, 1993). We found that deleting *DUN1* impaired checkpoint activation (60% arrested in G_2/M at 4 h after Gal-HO induction) (**Figure 4A**). The addition of an AID tag to Dun1 did not affect activation of the checkpoint (86% of cells arrested in G_2/M 4 h after damage induction) (**Figure 4B**). Moreover, degradation of Dun1-AID 4 h after damage induction did not cause a significant change in the proportion of G_2/M arrested in these otherwise wild type cells, nor did it affect Rad53 phosphorylation (**Figure 4B**). When *CHK1* was deleted in the Dun1-AID strain, the addition of IAA 4 h after DSB induction triggered an exit from checkpoint arrest (**Figure 4C**). These results suggest that Dun1 is required for a robust checkpoint activation but is not required for maintenance.

Ddc2's role in maintaining arrest becomes dispensable in extended G_2/M arrest

Previously we reported that Ddc2 protein abundance increases over time as the DDC is maintained and then decreased about the time that a strain with 1-DSB adapts (Memisoglu et al., 2019). Here we examined the levels of Ddc2 in both 1 and 2-DSB backgrounds and found that the level of Ddc2 modestly increased for the first 12 h after damage induction and then Ddc2 levels gradually declined with similar kinetics, but not falling below initial levels until 15 h after Gal-HO induction (**Figure 5A-C**). The drop in Ddc2 abundance coincides with the time that 1-DSB cells adapted, as measured by observing single cells on a YEP-Gal plate (**Figure 1A**). However, the 2-DSB strain remained arrested (**Figure 1D**) even though Ddc2 levels decreased to a comparable level (**Figure 5C**).

If Ddc2 activity is required to maintain arrest in the 2-DSB strain, then degradation of

Ddc2-AID 15 h after damage induction should trigger checkpoint release. While Ddc2-AID was readily degraded 15 h after HO induction and Rad53 phosphorylation diminished, there was no significant change in the percentage of G_2/M arrested cells even 9 h after having added auxin. (**Figure 5D; compare with Figure 2A, when IAA was added at 4 h**). DAPI staining showed that degradation of Ddc2-AID did not lead to cells progressing into anaphase, as >90% of cells remained in G_2/M with a single DAPI focus (**Figure 5F**). Therefore, while Ddc2 activity is required for the initial maintenance of checkpoint arrest, it is not required for prolonged arrest following 2 DSBs. These results suggest that another system takes over the maintenance of cell cycle arrest from the DDC by 15 h after induction of the DSBs.

Spindle Assembly Checkpoint Proteins Mad2 and Mad1 are Required for prolonged arrest

In addition to the DDC, the spindle assembly checkpoint (SAC) maintains genomic integrity by halting mitosis at the metaphase/anaphase transition to ensure accurate chromosome segregation (reviewed by (Amon, 1999). We have previously shown that inactivation of the SAC by a *MAD2* or *MAD1* deletion shortens checkpoint arrest in a 1-DSB strain from 15 h to 10 h (Dotiwala et al., 2010). To measure the contribution of the SAC in maintaining checkpoint arrest, we deleted *MAD2* in the 2-DSB strain. When G_1 cells were placed on YEP-Gal plates, nearly 100% of *mad2*Δ cells arrested 4 h but began to adapt between 12-15 h (**Figure S6B**). The prolonged arrest of 1- and 2-DSB strains when Ddc2 was overexpressed was dependent on Mad2 (**Figure S6A**). Based on these data we concluded that the handoff of checkpoint arrest from the DDC to the SAC likely occurs around 12-15 h after DSB-induction.

If Mad2 is not required for checkpoint activation, then degradation of Mad2-AID before 15 h, when 2-DSB *mad2*Δ cells begin to adapt, should not affect the percentage of G_2/M arrested

cells. We added IAA to Mad2-AID to cultures 4 h after DSB induction and found that the percentage of G_2/M cells did not significantly change between the split cultures until 14 h after adding IAA (18 h after DSB induction) (**Figure S7A**). Western blot analysis showed that Mad2-AID readily degraded with IAA treatment, but that Rad53 remained hyperphosphorylated at least through 24 h after DSB induction (**Figure S7B**). While the percentage G2/M-arrested Mad2-AID cells treated with IAA was significantly lower than untreated cells 24 h after DSB induction (57% vs. 78%) (**Figure S7, Table S1**), this fraction was substantially higher than the 3% percentage of *mad2*Δ cells that remained in G_2/M arrest in an adaptation assay after 24 h (**Figure S6B**).

To address this discrepancy in the percentage of G_2/M arrested cells between the *mad2*Δ adaptation assay and the morphology assay in a liquid culture with Mad2-AID + IAA, we developed a hybrid IAA-plating assay where DSBs were first induced in a liquid culture and after 4 h cells were plated on a YEP-Gal ± 1mM IAA plates for morphology measurements. An advantage of measuring morphology in this hybrid IAA-plating assay is that when a cell adapts on a plate it forms a microcolony that can be counted as a single adaptation event. Mad2-AID and Mad1-AID cells remained in arrest for up to 20 h on the YEP-Gal plate (without auxin) whereas cells began to adapt after 8 h on the YEP-Gal-IAA plate (**Figure S7C-D**). Western blot analysis from cells cultured in liquid medium showed that Mad1-AID readily degraded with IAA treatment and that Rad53 remained hyperphosphorylated up to 24 h after DSB induction (**Figure S7D**). This result reinforces our conclusion that Mad2 and Mad1 are not required for the activation and initial maintenance of arrest but are required later for checkpoint maintenance in response to 2 DSBs.

Handoff of checkpoint arrest from the DDC to the SAC

Degradation of Mad2-AID or Mad1-AID 15 h after DSB induction resulted in a reduction in G_2/M

arrested cells (**Figure 6A-B**). This release from checkpoint arrest occurred despite Rad53 remaining hyperphosphorylated (**Figure 6A-B**). DAPI staining of Mad2-AID and Mad1-AID cells from 15 h to 24 h after DSB induction showed an increase in the percentage of large-budded cells with 2 DAPI foci when auxin is added (**Figure S10A-B**).

If there is a complete handoff from the DDC to the SAC to maintain checkpoint arrest in the 2-DSB strain, then degrading Ddc2 and Mad2 after the handoff should not result in a decrease of G_2/M arrested cells compared with deactivating Mad2 alone. Using a Ddc2-AID Mad2-AID double mutant in a 2-DSB strain, we added IAA at 15 h. Although Ddc2-AID was readily degraded and Rad53 was dephosphorylated (**Figure S8A**), morphology analysis by the IAA-plating assay showed that there was no significant difference in the percentage of cells escaping G_2/M arrest when IAA was added 15 h after Gal-HO induction to the Mad2-AID and the double mutant Ddc2-AID Mad2-AID (**Figure S8A-B and Table 1**). The data suggests that the maintenance of prolonged checkpoint arrest after two double-strand breaks becomes independent of the Rad53 phosphorylation state once the DDC hands over the control to the SAC.

Mitotic exit network proteins Bfa1 and Bub2 have different roles in the DDR

In a previous study, we demonstrated that deleting *BUB2* shortened DSB-induced checkpoint arrest in a strain with one DSB (Dotiwala et al., 2010). To investigate the role of Bub2 and Bfa1, which are involved in the mitotic exit network (MEN), in maintaining arrest with two DSBs, we used AID-tagged Bub2 and Bfa1 strains. We repeated the IAA-plating assay and DAPI staining, exposing cells to IAA at 4 h and 15 h after DSB induction. Bub2-AID behaved similarly to Mad2-AID and Mad1-AID when treated with IAA at 4 h and 15 h after DSB induction (**Figure 6C, S9A-B, and S10C**). However, Bfa1-AID degradation did not trigger a significant release from

checkpoint arrest, and Rad53 remained hyperphosphorylated in both cases (**Figure 6D, S9C-D, and S10D**). Importantly, neither the inactivation of Bub2 nor Bfa1 led to cells completing anaphase and displaying two DAPI-stained nuclei, which is the phenotype of arrest at mitotic exit. These results suggest that Bub2 may have a Bfa1-independent role in checkpoint arrest.

Discussion

The DNA damage checkpoint (DDC) plays a crucial role in preventing damaged chromosomes from propagating in future generations. In our study, we utilized the auxin-inducible degron (AID) system to investigate how the DDC is maintained after activation. We found most of the signaling proteins activated by the DDC must remain activated until the repair is complete or adaptation occurs, highlighting the importance of continuous maintenance in preventing genomic instability

Phosphorylation of Rad53 by Mec1 is tightly linked to cell cycle arrest following DNA damage (Pellicioli et al., 2001). While Rad53 is also phosphorylated by Tel1, deletion of *TEL1* did not affect the >24 h checkpoint arrest in a 2 DSB strain. Mec1 activation in the S and G_2 cell cycle phases is achieved by at least two converging mechanisms; first, through Ddc2 binding to RPA-coated ssDNA and second, through direct activation by the 9-1-1 clamp subunit Ddc1 (Dubrana et al., 2007; Navadgi-Patil and Burgers, 2009; Zou and Elledge, 2003). In agreement with previous results regarding direct Mec1 inhibition (Pellicioli et al., 2001; Vaze et al., 2002), degradation of Ddc2 4 h after checkpoint activation results in the rapid resumption of the cell cycle. While degradation of Ddc2 in this context does not necessarily directly inhibit Mec1 activity, the loss of Rad53 phosphorylation upon Ddc2 degradation suggests that Mec1 is indeed deactivated and that dephosphorylation of Rad53 is a constitutive, competing event to Rad53's phosphorylation (Leroy et al., 2003).

Before Ddc1 can activate Mec1, the 9-1-1 clamp must be loaded by the clamp loader, which consists of Rad24-Rfc2-5 (Melo et al., 2001). Checkpoint activation largely depends on a functional clamp loader as cells lacking *RAD24* proceed through mitosis with only a brief delay (Aylon and Kupiec, 2003). If the clamp loader acts just once to load the 9-1-1 clamp and slides away from the DSB as it is being resected, then removal of Rad24 after the checkpoint has been robustly activated should not perturb arrest. However, we found that degradation of Rad24 rapidly leads to cell cycle resumption in response to two DSBs, suggesting the requirement for multiple 9-1-1 clamp loading events to sustain the checkpoint's maintenance. There may be continuous loading and unloading as the 3' end also is engaged by Exo1 and Sgs1-Rmi1-Top3-Dna2 exonucleases (Zhu et al., 2008).

Rad9, downstream of Mec1 and Tel1, is responsible for scaffolding the activation of the checkpoint kinases Rad53 and Chk1 (Emili, 1998; Schwartz et al., 2002; Sweeney et al., 2005). Degradation of Rad9 terminates checkpoint signaling with respect to both cell cycle arrest and Rad53 phosphorylation. This demonstrates that, in addition to its role in the initial Rad53 phosphorylation, Rad9 is also required for maintenance of Rad53 phosphorylation.

We further showed that Rad53 degradation triggers releases cells from G2/M arrest, albeit delayed by 4 h compared to degradation of the more upstream checkpoint components: Ddc2, Rad9, or Rad24. This residual checkpoint delay is apparently due to Chk1 signaling, as deleting Chk1 abrogates the 4 h delay. Since Chk1 directly inhibits mitosis by phosphorylating and stabilizing Pds1 (Agarwal et al., 2003), it is possible that the residual checkpoint delay is due to this constraint.

Unlike other checkpoint activation proteins examined in this study, degradation of Dun1 4 h after DSB induction did not lead to checkpoint release. Possibly, once Dun1 has activated a

damage-related transcription response, the proteins produced are stable for several hours. In the DDC Dun1 has 2 known roles, the upregulation of damage-responsive genes such as *HUG1* and *RNR3,* which increases dNTP production (Zhao and Rothstein, 2002; Zhou and Elledge, 1993), and prevention of the onset of anaphase by binding to the E3 ligase Rsp5 to prevent degradation of the securin Pds1 (Yam et al., 2020). Our results show that Dun1 activity is required for optimal checkpoint activation, but not required for maintenance in the presence of Chk1.

There is also evidence that SAC proteins contribute to the DNA damage response. We have shown that engagement of the SAC by a DSB occurs in *cis* (that is, on the same chromosome that suffers the DSB) when the γ-H2AX modification spreads to the centromere (Dotiwala et al., 2010). This finding suggests that DDC and the SAC contribute to DSB-induced checkpoint arrest through different pathways, but in the case of an HO-induced break there seems instead to be a direct handoff from the DDC to the SAC.

Here, we directly show that the >24 h arrest following induction of 2 DSBs is dependent on Mad2 and Mad1. Degradation of Mad2 or Mad1 4 h after DSB induction did not immediately result in checkpoint release, but cells begin to resume cell cycle progression 15 h after DSB induction and by 24 h most cells had escaped checkpoint arrest. Although cells escaped checkpoint arrest when Mad2 or Mad1 were degraded, the distribution of cell types did not return to pre-damage levels in a liquid culture, which could be due to a change in the length of cell cycle phases. Simultaneous degradation of Ddc2 and Mad2 at 15 h resulted in no difference in the percentage of cells in G_2/M arrest compared with the degradation of Mad2 alone. Surprisingly, in the absence of Mad1 or Mad2 cells escaped arrest, despite Rad53 remaining hyperphosphorylated up to 24 h. While overexpression of Ddc2 can maintain checkpoint arrest for >24 h following 1- or 2- DSBs, this arrest still requires Mad2. The reason why Rad53 activity is not sufficient to maintain arrest

>24 hours is unknown.

In addition to blocking the metaphase to anaphase transition, the DDC also blocks mitotic exit (reviewed in (Matellan and Monje-Casas, 2020)). To look at the role of the mitotic exit network (MEN) in checkpoint maintenance, we examined the 2 most upstream components of the MEN pathway, the heterodimer Bub2/Bfa1 which binds to Tem1 to prevent the initiation of the mitotic exit network (MEN) (Matellan and Monje-Casas, 2020). Phosphorylation of Bfa1 by Cdc5 weakens the binding of Bfa1/Bub2 to Tem1 to trigger the activation of the MEN pathway (Hu et al., 2001). Much like Mad2 and Mad1, we found that neither Bub2 nor Bfa1 was required for the establishment of checkpoint arrest through the DDC. Our findings reveal a surprising result: S Bub2, but not its partner Bfa1, is required to prolong checkpoint arrest indicating that Bub2 has a role independent of Bfa1-in maintaining prolonged checkpoint arrest. Notably, Bfa1 is modified by the DDC factors Chk1, Rad53, and Dun1 which is thought to control mitotic exit (Hu et al., 2001). In the case of telomere damage, Rad53 prevents Bfa1 phosphorylation by phosphorylating Cdc5 (Valerio-Santiago et al., 2013). Collectively, our results highlight the importance of the SAC in sustaining prolonged or permanent arrest in response to DSBs.

Methods and Materials

Yeast strain and plasmid construction

All AID-tagged mutants strains were derived from a modified version of JKM179 (DW417) expressing osTIR1 integrated at *URA3* after cutting pNHK53 (Nishimura et al., 2009) with *Stu*I to target the integration. To create the strain with two HO cleavage sites (DW417), the HO cut site with the HPH marker was integrated into chromosome 6, 52 kb from the centromere, in DW18. To create degron tagged derivatives, PCR products were generated with mixed oligos with homology

to the C-terminal end of the open reading frame and plasmids pKan–AID*–9myc (pJH2892) or pNat–AID*–9myc (pJH2899) (Morawska and Ulrich, 2013) to create an AID-9xMyc (AID) insert with KAN or NAT markers. Deletion of ORFs and AID tags were introduced with the one step PCR homology cassette amplification and the standard yeast transformation method (Wach et al., 1994). Transformants were verified by PCR and western blot. Strains are listed in **Table S2**. Primers are listed in **Table S3**. Plasmids are listed in **Table S4**.

Culturing conditions, HO expression, and auxin treatment

Strains containing degron fusions and galactose-inducible HO were cultured using standard procedures. Briefly, a single colony grown on a YPD plate was inoculated in 5 ml YEP-lactate for ~15 hours overnight at 30° C with agitation. The following day, 500-100 ml of YP-lactate was inoculated by this starter culture such that the cell density reached OD600 = 0.5 the following day after overnight growth at 30° C with agitation. HO expression was induced by addition of 20% galactose to 2% vol/vol final concentration. For auxin treatment, indole-3-acetic acid (IAA) was resuspended in ethanol to a concentration of 500 mM. Cultures were split 4 h or 15 h after adding galactose; either IAA (1mM) or an equivalent volume of 200 proof ethanol was added to split cultures. At indicated timepoints, 15 ml of culture were collected and prepared for microscopy or western blot analysis as described below.

TCA protein extraction

Protein extracts were prepared for western blot analysis by the standard TCA protocol (Miller-Fleming et al., 2014). Briefly, harvested cells were incubated on ice in 1.5ml microcentrifuge tubes with 20% TCA for 20 minutes. Cells were washed with acetone and pellet was air dried. 200ul of

MURBs buffer (50mM sodium phosphate, 25mM MES, 3M urea, 0.5% 2-mercaptoethanol, 1 mM sodium azide, and 1% SDS) was added to each sample with acid washed glass beads. Cells were lysed by mechanical shearing with glass beads for 2 minutes. Supernatant was collected by poking a hole in the bottom of the 1.5ml microcentrifuge tube and spun in a 15ml conical tube. Samples were boiled at 95C for 10 minutes.

Western blotting

8 – 20 µl of denatured protein samples prepared by TCA extraction were loaded into a 10% or 6% SDS page gel. Proteins were separated by applying 90 V constant until the 37 kDa marker reached the bottom of the gel. Gels were transferred to an Immun-Blot PVDF using a wet transfer apparatus set to 100 V constant voltage for 1 h at 4 °C. Membranes were then blocked with OneBlock blocking buffer (Genesee Scientific Cat #: 20-313) for 1 h at room temperature. After 3 washes with 1x TBS-T, blots were incubated with either anti-Myc [9E11] (Abcam, ab56) to detect TIR1 and AID fusions, anti-Rad53 [EL7.E1] (Abcam, ab166859), or anti-Pgk1 (Abcam, ab30359) for 1 h at room temperature. Reagents used are in **Table S5**. Blots were washed 3 times with 1x TBS-T and incubated with anti-mouse HRP secondary antibody for 1 h at room temperature. After washing 3 times with 1x TBS-T, ECL Prime was added to fully coat the blots and left to incubate for 5 min at room temperature with gentle agitation. Blots were imaged using a BioRad ChemiDoc XR+ imager and prepared for publication using Image Lab software (BioRad) and Adobe Photoshop CC 2017.

Microscopy, DAPI staining, and cell morphology determination

Aliquots from YEP-Lac cultures were taken at specified timepoints and diluted to ~10^6 cells/ml.

10µl of each sample was placed on a hemocytometer and cells were counted on a light microscope with a 10x objective. Cells examined were binned into three categories: unbudded, small buds, and large buds (G_2/M arrested cells). For each timepoint >250 cells were analyzed. Graphs were prepared using GraphPad Prism. For DAPI staining, 450 µl of culture was added to 50 µl of 37% formaldehyde and incubated in the chemical hood at room temperature for 20 min. Samples were spun down at 8000 rpm for 5 min and washed with 1X PBS 3 times. Cells were resuspended in 50 µl of DAPI mounting media (VECTASHIELD® Antifade Mounting Medium with DAPI H-1200-10) and incubated at room temperature for 10 min away from direct light. Cells were imaged using a spinning disc microscope with a 358 nm laser.

Adaptation and auxin plating assays

The ability of cells to adapt was determined as previously described (Eapen et al., 2012; Lee et al., 1998). Overnight cultures in YEP-lactate were diluted 20-fold in sterile water and plated in a line down the center of a YEP-gal plate. Using micromanipulation, 50 G_1 cells were isolated and positioned in a grid followed by incubation at 30° C. The number of cells that grew to a microcolony (3+ cells) after 24 h was divided by the total number of cells, to give percent adaptation. For an auxin plating assay, damage was induced in a YEP-lactate culture by adding galactose (2%) as previously described. To degrade AID-tagged proteins, galactose+ cultures were then placed on a YEP-Gal plate or a YEP-Gal plate with 1 mM IAA as described above for an adaptation assay. Cell morphology was determined as previously described.

Competing Interest Statement

The authors declare no competing interests.

Acknowledgments

We are grateful to Helle Ulrich for donations of the AID and TIR1 plasmids. Research was supported by NIH grant R35 GM127029. D.P.W. and S.C.-P. were supported by NIH Genetics Training Grant TM32GM007122. V.V.E. was supported by the Howard Hughes Medical Institute International Predoctoral Fellowship. We also thank Nikita Alimov, Jessie Ang and Astré Bouchier for additional assistance.

Author Contributions

Conceptualization and initial data collection with Ddc2, Rad9, Rad24, Rad53, and Mad2 was conducted by David P. Waterman Vinay V. Eapen and James E. Haber. Experiments with Mad1, Bub2, and Bfa1; measuring Ddc2 levels; and DAPI staining was done by Felix Zhou. The manuscript was authored by Felix Zhou, David P. Waterman, and James E. Haber. Data collection, strain making, imaging, primer design, and data analysis were performed by Felix Zhou, David P. Waterman, and Suhaily Caban-Penix.

References

Agarwal, R., Tang, Z., Yu, H., and Cohen-Fix, O. (2003). Two distinct pathways for inhibiting pds1 ubiquitination in response to DNA damage. J Biol Chem *278*, 45027-45033.

Amon, A. (1999). The spindle checkpoint. Curr Opin Genet Dev *9*, 69-75.

Aylon, Y., and Kupiec, M. (2003). The checkpoint protein Rad24 of Saccharomyces cerevisiae is involved in processing double-strand break ends and in recombination partner choice. Mol Cell Biol *23*, 6585-6596.

Chen, S.H., Smolka, M.B., and Zhou, H. (2007). Mechanism of Dun1 activation by Rad53 phosphorylation in Saccharomyces cerevisiae. J Biol Chem *282*, 986-995.

Clemenson, C., and Marsolier-Kergoat, M.C. (2009). DNA damage checkpoint inactivation: adaptation and recovery. DNA repair *8*, 1101-1109.

de la Torre-Ruiz, M.A., Green, C.M., and Lowndes, N.F. (1998). RAD9 and RAD24 define two additive, interacting branches of the DNA damage checkpoint pathway in budding yeast normally required for Rad53 modification and activation. EMBO J *17*, 2687-2698.

Dotiwala, F., Haase, J., Arbel-Eden, A., Bloom, K., and Haber, J.E. (2007). The yeast DNA damage checkpoint proteins control a cytoplasmic response to DNA damage. Proc Natl Acad Sci U S A *104*, 11358-11363.
Dotiwala, F., Harrison, J.C., Jain, S., Sugawara, N., and Haber, J.E. (2010). Mad2 prolongs DNA damage checkpoint arrest caused by a double-strand break via a centromere-dependent mechanism. Curr Biol *20*, 328-332.
Dubrana, K., van Attikum, H., Hediger, F., and Gasser, S.M. (2007). The processing of double-strand breaks and binding of single-strand-binding proteins RPA and Rad51 modulate the formation of ATR-kinase foci in yeast. J Cell Sci *120*, 4209-4220.
Durocher, D., Henckel, J., Fersht, A.R., and Jackson, S.P. (1999). The FHA domain is a modular phosphopeptide recognition motif. Mol Cell *4*, 387-394.
Eapen, V.V., Sugawara, N., Tsabar, M., Wu, W.H., and Haber, J.E. (2012). The Saccharomyces cerevisiae chromatin remodeler Fun30 regulates DNA end resection and checkpoint deactivation. Mol Cell Biol *32*, 4727-4740.
Ellison, V., and Stillman, B. (2003). Biochemical characterization of DNA damage checkpoint complexes: clamp loader and clamp complexes with specificity for 5' recessed DNA. PLoS Biol *1*, E33.
Emili, A. (1998). MEC1-dependent phosphorylation of Rad9p in response to DNA damage. Mol Cell *2*, 183-189.
Fiorani, S., Mimun, G., Caleca, L., Piccini, D., and Pellicioli, A. (2008). Characterization of the activation domain of the Rad53 checkpoint kinase. Cell Cycle *7*, 493-499.
Garber, P.M., and Rine, J. (2002). Overlapping roles of the spindle assembly and DNA damage checkpoints in the cell-cycle response to altered chromosomes in Saccharomyces cerevisiae. Genetics *161*, 521-534.
Hu, F., Wang, Y., Liu, D., Li, Y., Qin, J., and Elledge, S.J. (2001). Regulation of the Bub2/Bfa1 GAP complex by Cdc5 and cell cycle checkpoints. Cell *107*, 655-665.
Kim, E.M., and Burke, D.J. (2008). DNA damage activates the SAC in an ATM/ATR-dependent manner, independently of the kinetochore. PLoS Genet *4*, e1000015.
Kim, J.A., Kruhlak, M., Dotiwala, F., Nussenzweig, A., and Haber, J.E. (2007). Heterochromatin is refractory to gamma-H2AX modification in yeast and mammals. J Cell Biol *178*, 209-218.
Lanz, M.C., Dibitetto, D., and Smolka, M.B. (2019). DNA damage kinase signaling: checkpoint and repair at 30 years. EMBO J *38*, e101801.
Lee, C.S., Lee, K., Legube, G., and Haber, J.E. (2014). Dynamics of yeast histone H2A and H2B phosphorylation in response to a double-strand break. Nat Struct Mol Biol *21*, 103-109.
Lee, S.E., Moore, J.K., Holmes, A., Umezu, K., Kolodner, R.D., and Haber, J.E. (1998). Saccharomyces Ku70, mre11/rad50 and RPA proteins regulate adaptation to G2/M arrest after DNA damage. Cell *94*, 399-409.
Leroy, C., Lee, S.E., Vaze, M.B., Ochsenbein, F., Guerois, R., Haber, J.E., and Marsolier-Kergoat, M.C. (2003). PP2C phosphatases Ptc2 and Ptc3 are required for DNA checkpoint inactivation after a double-strand break. Mol Cell *11*, 827-835.
Li, K., Bronk, G., Kondev, J., and Haber, J.E. (2020). Yeast ATM and ATR kinases use different mechanisms to spread histone H2A phosphorylation around a DNA double-strand break. Proc Natl Acad Sci U S A *117*, 21354-21363.

Limbo, O., Porter-Goff, M.E., Rhind, N., and Russell, P. (2011). Mre11 nuclease activity and Ctp1 regulate Chk1 activation by Rad3ATR and Tel1ATM checkpoint kinases at double-strand breaks. Mol Cell Biol *31*, 573-583.
Majka, J., Binz, S.K., Wold, M.S., and Burgers, P.M. (2006). Replication protein A directs loading of the DNA damage checkpoint clamp to 5'-DNA junctions. J Biol Chem *281*, 27855-27861.
Mantiero, D., Clerici, M., Lucchini, G., and Longhese, M.P. (2007). Dual role for Saccharomyces cerevisiae Tel1 in the checkpoint response to double-strand breaks. EMBO Rep *8*, 380-387.
Marangos, P., Stevense, M., Niaka, K., Lagoudaki, M., Nabti, I., Jessberger, R., and Carroll, J. (2015). DNA damage-induced metaphase I arrest is mediated by the spindle assembly checkpoint and maternal age. Nat Commun *6*, 8706.
Marechal, A., and Zou, L. (2015). RPA-coated single-stranded DNA as a platform for post-translational modifications in the DNA damage response. Cell Res *25*, 9-23.
Matellan, L., and Monje-Casas, F. (2020). Regulation of Mitotic Exit by Cell Cycle Checkpoints: Lessons From Saccharomyces cerevisiae. Genes (Basel) *11*.
Melo, J.A., Cohen, J., and Toczyski, D.P. (2001). Two checkpoint complexes are independently recruited to sites of DNA damage in vivo. Genes Dev *15*, 2809-2821.
Memisoglu, G., Lanz, M.C., Eapen, V.V., Jordan, J.M., Lee, K., Smolka, M.B., and Haber, J.E. (2019). Mec1(ATR) Autophosphorylation and Ddc2(ATRIP) Phosphorylation Regulates DNA Damage Checkpoint Signaling. Cell Rep *28*, 1090-1102 e1093.
Miller-Fleming, L., Cheong, H., Antas, P., and Klionsky, D.J. (2014). Detection of Saccharomyces cerevisiae Atg13 by western blot. Autophagy *10*, 514-517.
Moore, J.K., and Haber, J.E. (1996). Cell cycle and genetic requirements of two pathways of nonhomologous end-joining repair of double-strand breaks in Saccharomyces cerevisiae. Mol Cell Biol *16*, 2164-2173.
Morawska, M., and Ulrich, H.D. (2013). An expanded tool kit for the auxin-inducible degron system in budding yeast. Yeast *30*, 341-351.
Musacchio, A., and Salmon, E.D. (2007). The spindle-assembly checkpoint in space and time. Nat Rev Mol Cell Biol *8*, 379-393.
Navadgi-Patil, V.M., and Burgers, P.M. (2009). The unstructured C-terminal tail of the 9-1-1 clamp subunit Ddc1 activates Mec1/ATR via two distinct mechanisms. Mol Cell *36*, 743-753.
Nishimura, K., Fukagawa, T., Takisawa, H., Kakimoto, T., and Kanemaki, M. (2009). An auxin-based degron system for the rapid depletion of proteins in nonplant cells. Nat Methods *6*, 917-922.
Paciotti, V., Clerici, M., Lucchini, G., and Longhese, M.P. (2000). The checkpoint protein Ddc2, functionally related to S. pombe Rad26, interacts with Mec1 and is regulated by Mec1-dependent phosphorylation in budding yeast. Genes Dev *14*, 2046-2059.
Pellicioli, A., Lee, S.E., Lucca, C., Foiani, M., and Haber, J.E. (2001). Regulation of Saccharomyces Rad53 checkpoint kinase during adaptation from DNA damage-induced G2/M arrest. Mol Cell *7*, 293-300.
Pellicioli, A., Lucca, C., Liberi, G., Marini, F., Lopes, M., Plevani, P., Romano, A., Di Fiore, P.P., and Foiani, M. (1999). Activation of Rad53 kinase in response to DNA damage and its effect in modulating phosphorylation of the lagging strand DNA polymerase. EMBO J *18*, 6561-6572.
Sanchez, Y., Bachant, J., Wang, H., Hu, F., Liu, D., Tetzlaff, M., and Elledge, S.J. (1999). Control of the DNA damage checkpoint by chk1 and rad53 protein kinases through distinct mechanisms. Science *286*, 1166-1171.

Schwartz, M.F., Duong, J.K., Sun, Z., Morrow, J.S., Pradhan, D., and Stern, D.F. (2002). Rad9 phosphorylation sites couple Rad53 to the Saccharomyces cerevisiae DNA damage checkpoint. Mol Cell *9*, 1055-1065.
Sweeney, F.D., Yang, F., Chi, A., Shabanowitz, J., Hunt, D.F., and Durocher, D. (2005). Saccharomyces cerevisiae Rad9 acts as a Mec1 adaptor to allow Rad53 activation. Curr Biol *15*, 1364-1375.
Tsabar, M., Eapen, V.V., Mason, J.M., Memisoglu, G., Waterman, D.P., Long, M.J., Bishop, D.K., and Haber, J.E. (2015). Caffeine impairs resection during DNA break repair by reducing the levels of nucleases Sae2 and Dna2. Nucleic Acids Res *43*, 6889-6901.
Usui, T., and Petrini, J.H. (2007). The Saccharomyces cerevisiae 14-3-3 proteins Bmh1 and Bmh2 directly influence the DNA damage-dependent functions of Rad53. Proc Natl Acad Sci U S A *104*, 2797-2802.
Valerio-Santiago, M., de Los Santos-Velazquez, A.I., and Monje-Casas, F. (2013). Inhibition of the mitotic exit network in response to damaged telomeres. PLoS Genet *9*, e1003859.
Vaze, M.B., Pellicioli, A., Lee, S.E., Ira, G., Liberi, G., Arbel-Eden, A., Foiani, M., and Haber, J.E. (2002). Recovery from checkpoint-mediated arrest after repair of a double-strand break requires Srs2 helicase. Mol Cell *10*, 373-385.
Wach, A., Brachat, A., Pohlmann, R., and Philippsen, P. (1994). New heterologous modules for classical or PCR-based gene disruptions in Saccharomyces cerevisiae. Yeast *10*, 1793-1808.
Waterman, D.P., Haber, J.E., and Smolka, M.B. (2020). Checkpoint Responses to DNA Double-Strand Breaks. Annu Rev Biochem *89*, 103-133.
Yam, C.Q.X., Chia, D.B., Shi, I., Lim, H.H., and Surana, U. (2020). Dun1, a Chk2-related kinase, is the central regulator of securin-separase dynamics during DNA damage signaling. Nucleic Acids Res *48*, 6092-6107.
Zhao, X., and Rothstein, R. (2002). The Dun1 checkpoint kinase phosphorylates and regulates the ribonucleotide reductase inhibitor Sml1. Proc Natl Acad Sci U S A *99*, 3746-3751.
Zhou, Z., and Elledge, S.J. (1993). DUN1 encodes a protein kinase that controls the DNA damage response in yeast. Cell *75*, 1119-1127.
Zhu, Z., Chung, W.H., Shim, E.Y., Lee, S.E., and Ira, G. (2008). Sgs1 helicase and two nucleases Dna2 and Exo1 resect DNA double-strand break ends. Cell *134*, 981-994.
Zou, L., and Elledge, S.J. (2003). Sensing DNA damage through ATRIP recognition of RPA-ssDNA complexes. Science *300*, 1542-1548.

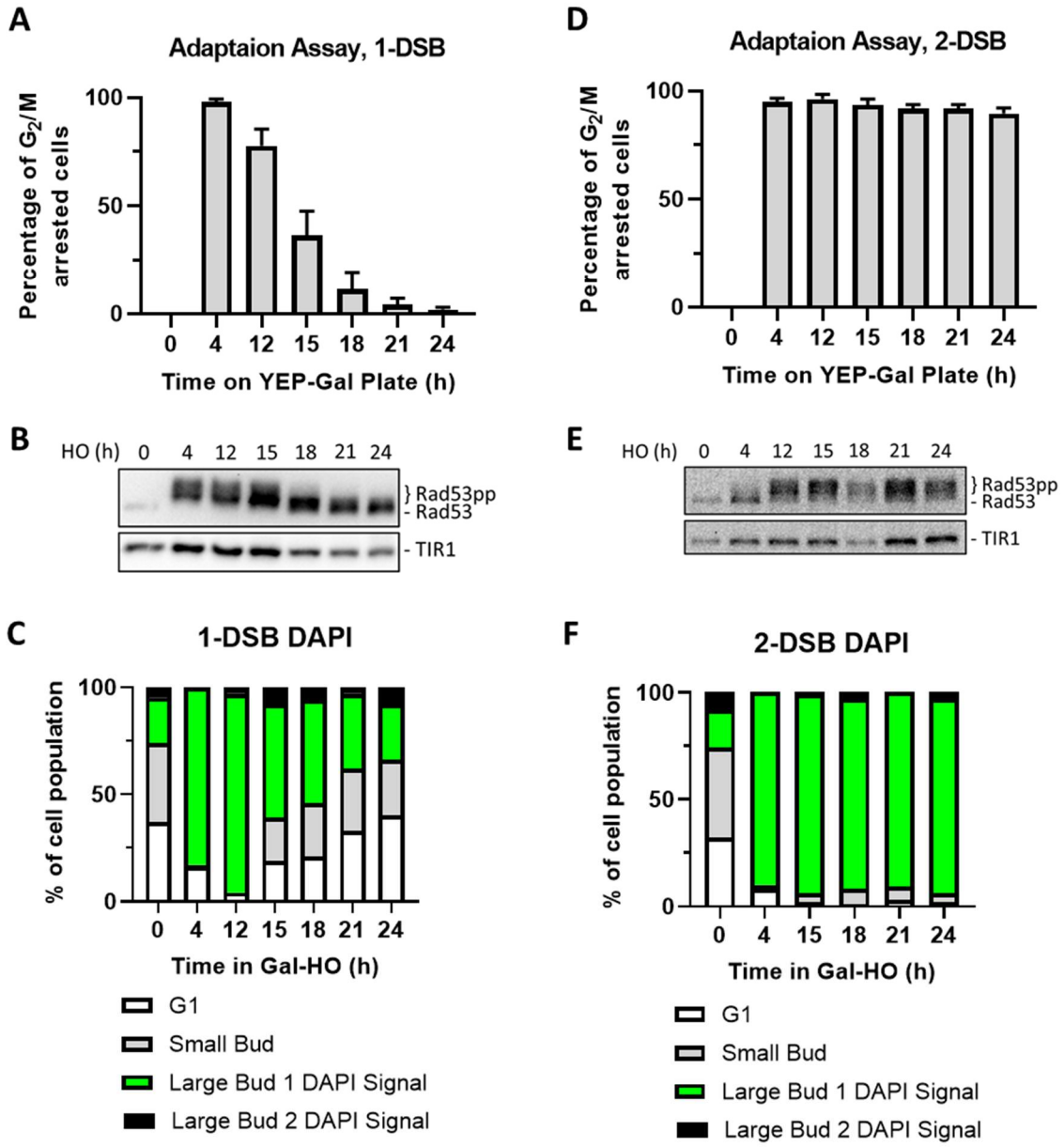

Figure 1. Measuring checkpoint arrest in a 1-DSB and 2-DSB strain
(A) Adaptation assay of 50 G_1 cells on a YEP-Gal plate with 1-DSB. G_2/M arrest was determined based on cell morphology as shown in **Figure S1**. Data are shown from 3 trials with standard error of the mean (SEM). (B) Western blot probed with α-Rad53 in a 1-DSB strain. α-Rad53 shows both an unphosphorylated protein and multiple phosphorylated species. α-Myc was probed for TIR1 as a loading control.(C) Profile of DAPI stained cells in a 1-DSB strain after HO induction in liquid culture. Cells were grouped based on cell morphology and number of DAPI foci. (D) Same as (A) for a 2-DSB strain. (E) Same as (B) for a 2-DSB strain. (F) Same as (C) for a 2-DSB strain. Note: data from liquid cultures are shown with green bars, while data from YEP-GAL plates are shown with red bars.

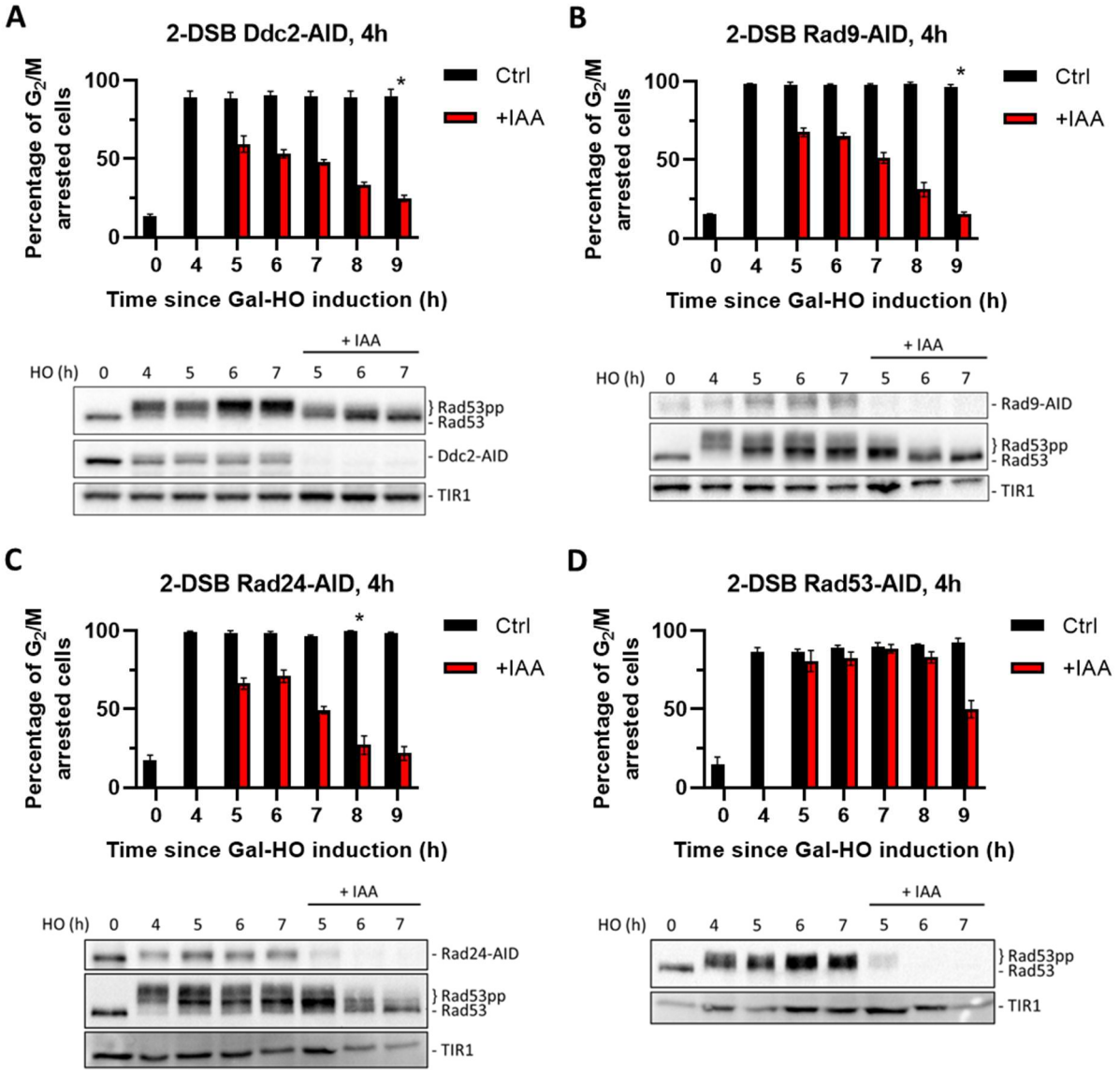

Figure 2. Checkpoint Maintenance Requires Ddc2, Rad9, Rad24, and Rad53 Activity
(A) Percentage of G_2/M arrested cells in a 2-DSB Ddc2-AID strain after Gal-HO induction in a liquid culture. Cultures were split 4 h after Gal-HO induction and either auxin (1mM) (+ IAA) or an equivalent volume of 200 proof ethanol was added. Data are shown from 3 trials with standard error of the mean (SEM). The asterisk shows when the percentage of large-budded cells returned to pre-damage levels. Western blot probed with α-Rad53 and α-Myc. α-Rad53 shows both an unphosphorylated protein and multiple phosphorylated species. α-Myc shows Ddc2-AID degradation and TIR1 as a loading control.(B) Same as (B) for 2-DSB Rad9-AID. (C) Same as (B) for 2-DSB Rad24-AID. (D) Same as (B) for 2-DSB Rad53-AID.

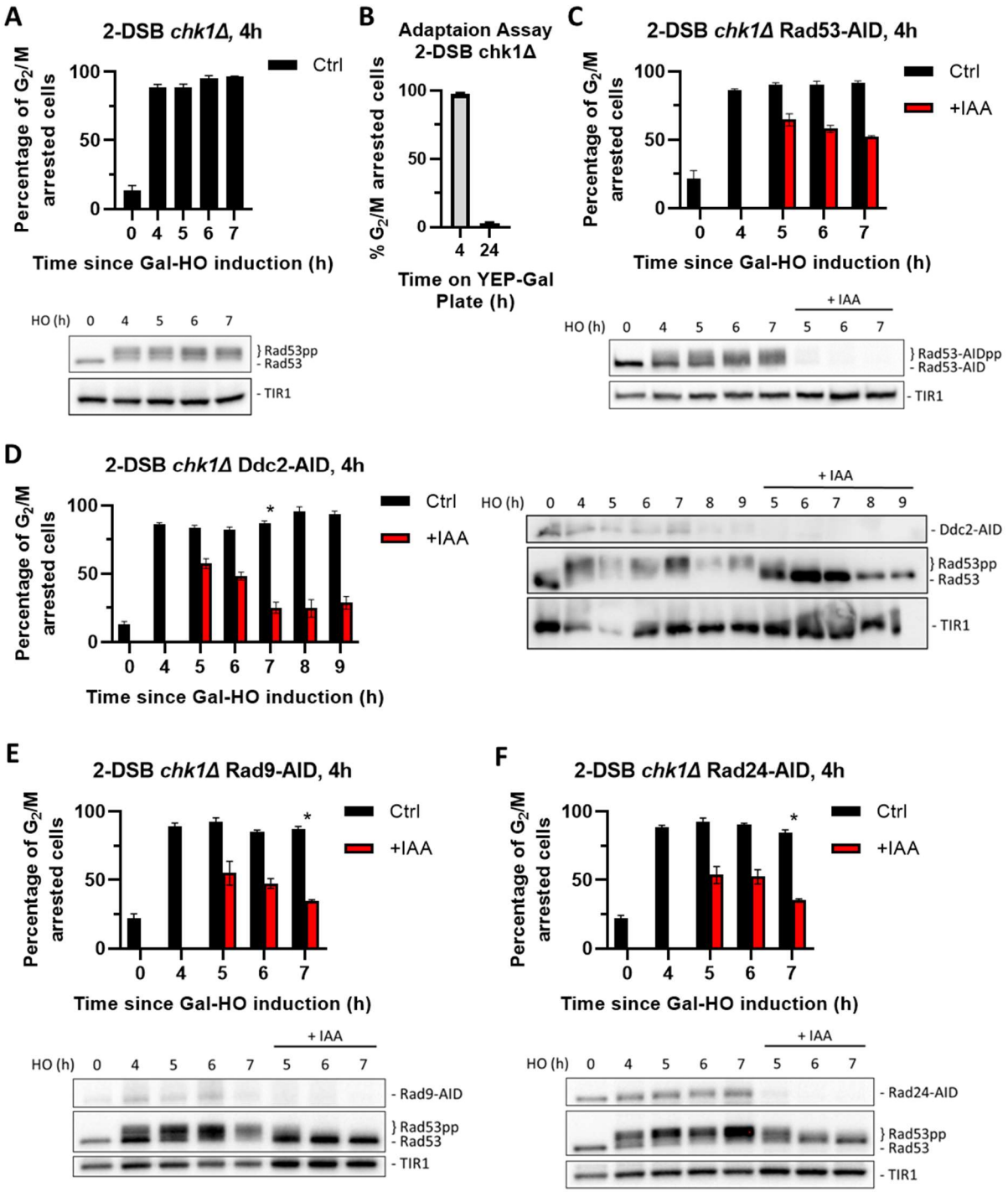

Figure 3. Chk1 is not Required for Checkpoint Activation

(A) Percent G_2/M cells in a 2-DSB *chk1*Δ strain after HO induction. Data are shown from 3 trials with standard error of the mean (SEM). Western blot probed with α-Rad53 and α-Myc. α-Rad53 shows both an unphosphorylated protein and multiple phosphorylated species. α-Myc shows TIR1 as a loading control. (B) Adaptation assay for 2-DSB *chk1*Δ strain. (C) Percentage of G_2/M arrested cells a 2-DSB *chk1*Δ Rad53-AID strain after HO induction. Cultures were split 4 h after DSB induction and 1 mM auxin (+IAA). Data are shown from 3 trials with standard error of the mean

(SEM). Western blot probed with α-Myc for Rad53-AID and TIR1 as a loading control. (D) Same as (C) for 2-DSB *chk1*Δ Ddc2-AID. Western blot probed with α-Rad53 and α-Myc. α-Rad53 shows both an unphosphorylated protein and multiple phosphorylated species. α-Myc shows Ddc2-AID degradation and TIR1 as a loading control. The asterisk shows when the percentage of large-budded cells returned to pre-damage levels. (E) Same as (D) for 2-DSB *chk1*Δ Rad9-AID. (F) Same as (D) for 2-DSB *chk1*Δ Rad24-AID.

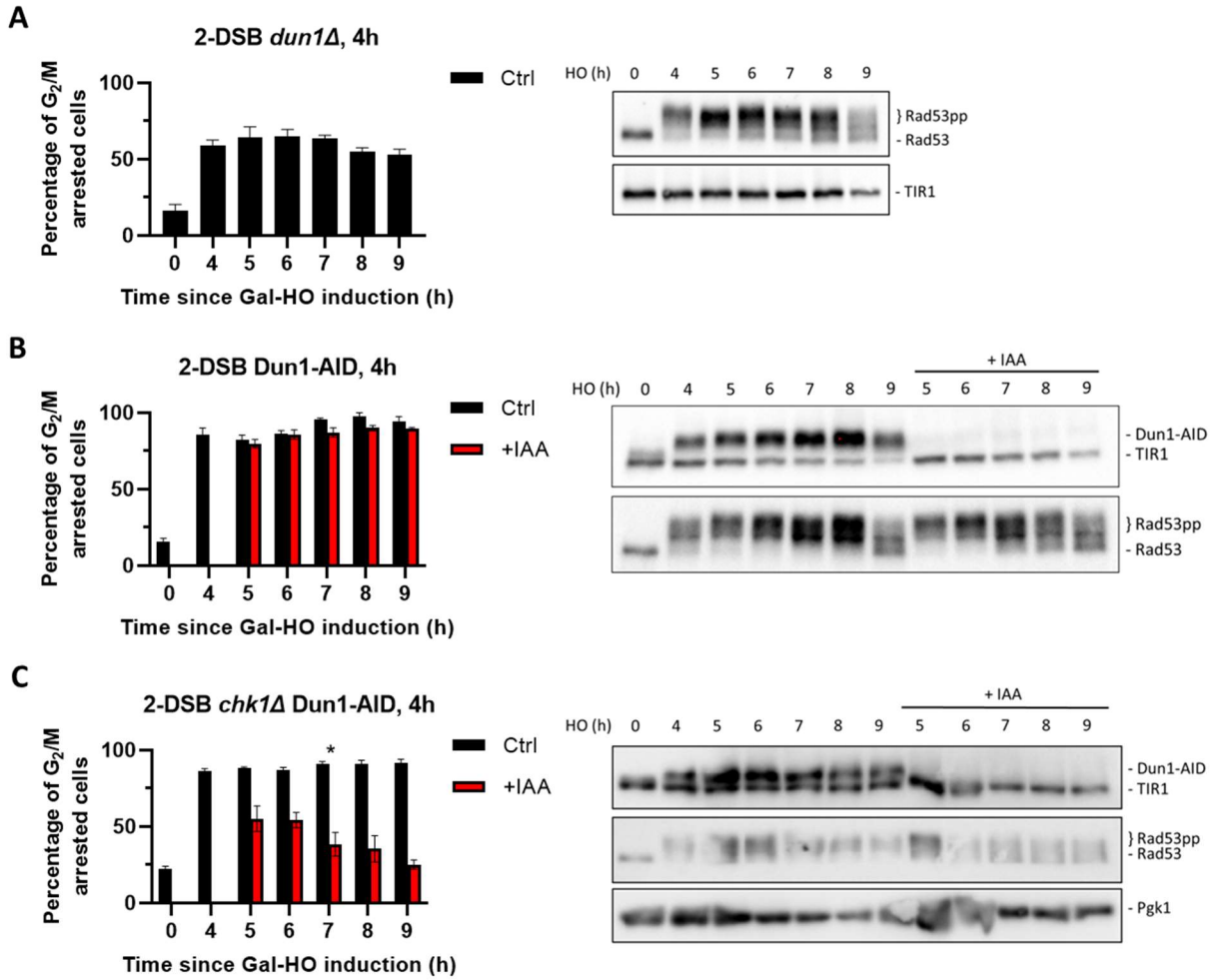

Figure 4. Dun1 is not Required for Checkpoint Maintenance
(A) Percent G_2/M arrested cells for 2-DSB *dun1*Δ after HO induction. Data are shown from 3 trials with standard error of the mean (SEM). Western blot probed with α-Rad53 and α-Myc for TIR1 as a loading control. (B) Percent G_2/M arrested cells for 2-DSB Dun1-AID after HO induction. Data are shown from 3 trials with standard error of the mean (SEM). Cultures were split 4 h after DSB induction; with auxin (1 mM) (+IAA). Western blot probed with α-Rad53 and α-Myc. α-Rad53 shows both an unphosphorylated protein and multiple phosphorylated species. α-Myc shows Dun1-AID degradation and TIR1 as a loading control. (C) Same as (B) for 2-DSB *chk1*Δ Dun1-AID. The asterisk marks when the percentage of large-budded cells returned to pre-damage levels.

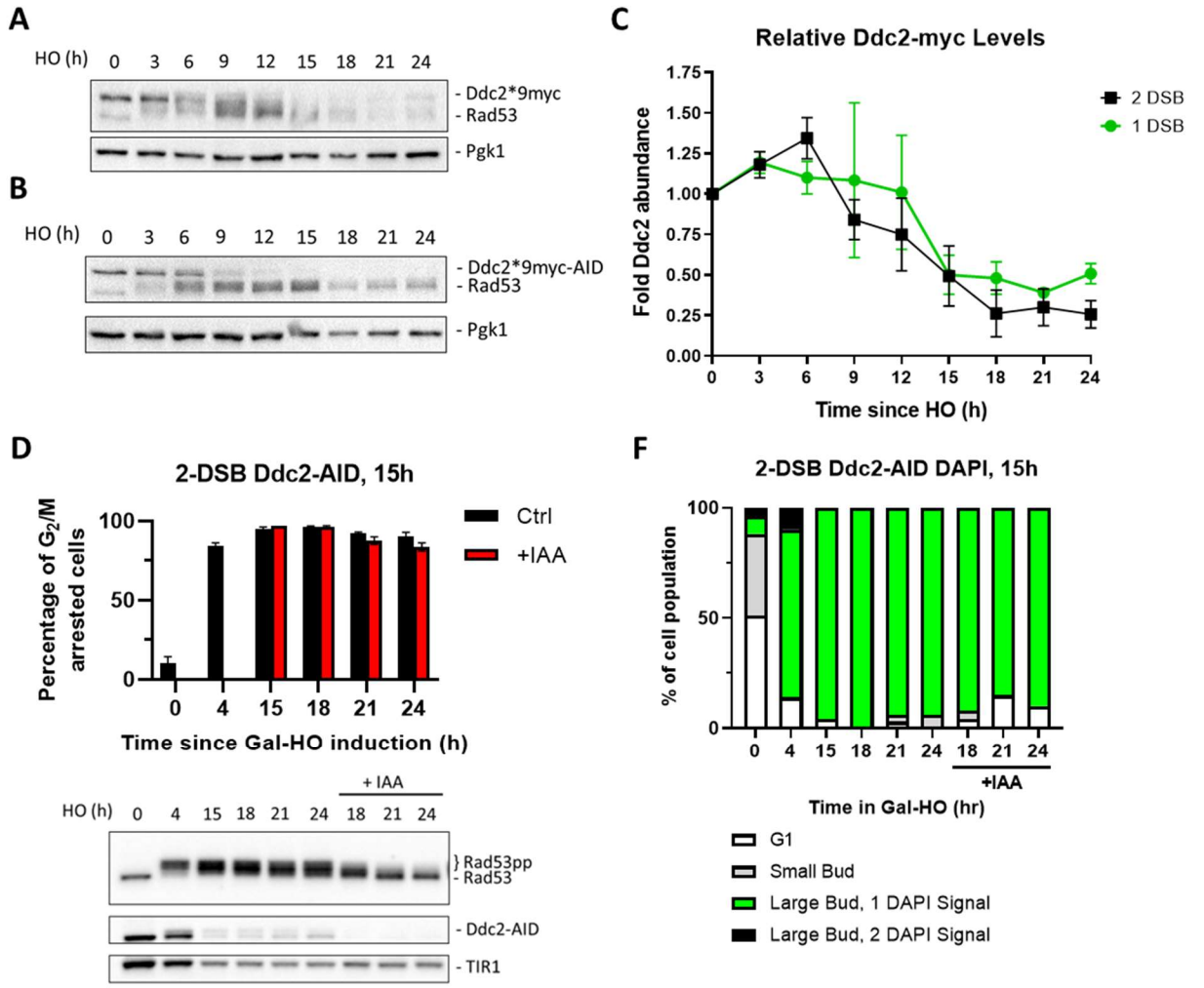

Figure 5. Relative levels of Ddc2 levels decrease after DSB induction.
(A-B) Western blots probed with α-Myc for Ddc2-9xMyc and Ddc2-9xMyc-AID in a 1-DSB and 2-DSB respectively. α-Pgk1 is used as a loading control. (C) Relative levels of Ddc2 in a 1-DSB and 2-DSB strain up to 24 h after DSB induction. (D) Percent G_2/M arrested cells for 2-DSB Ddc2-AID strain after HO induction. Cultures were split 15 h after DSB induction; with auxin (1mM) (+IAA). Data are shown from 3 trials with standard error of the mean (SEM). Western blot probed with α-Rad53 and α-Myc. α-Rad53 shows both an unphosphorylated protein and multiple phosphorylated species. α-Myc shows Ddc2-AID degradation and TIR1 as a loading control. (F) Profile of DAPI stained cells in a 2-DSB Ddc2-AID strain after HO induction. Cells were categorized based on cell morphology and number of DAPI signals.

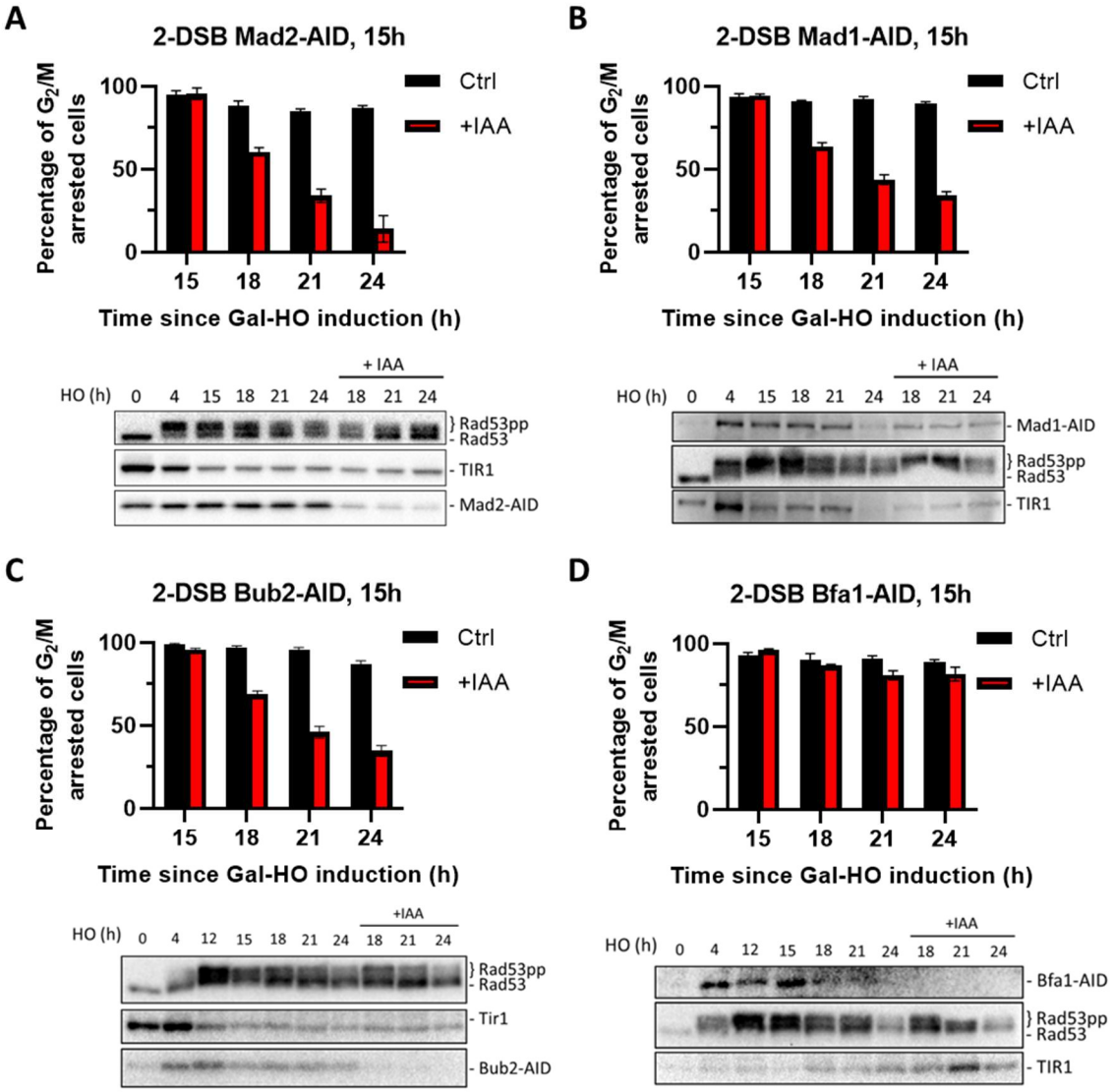

Figure 6. Degradation of Mad2, Mad1, or Bub2 at 15 h Releases Cells from Checkpoint Arrest but not Bfa1

(A) Percent G_2/M arrested cells for 2-DSB Mad2-AID after HO induction. Data is shown from 3 trials with standard error of the mean (SEM). Western blot probed with α-Rad53 and α-Myc. α-Rad53 shows both an unphosphorylated protein and multiple phosphorylated species. α-Myc shows Mad2-AID degradation and TIR1 as a loading control. (B) Same as (A) for 2-DSB Mad1-AID. (C) Same as (A) for 2-DSB Bub2-AID. (D) Same as (A) for 2-DSB Bfa1-AID.